Comparison of joining efficiency and residual stresses in laser and laser hybrid welding

W. Suder, S. Ganguly, S. Williams, A.M. Paradowska, P. Colegrove

Abstract

Laser welding is a high energy density process, which can produce welds with less energy input and thereby, lower residual stress generation compared to arc welding processes. However, the narrow beam dimension makes it extremely sensitive in terms of fit up tolerance. This causes problem in achieving high quality welds. Laser with arc hybrid process overcomes such issues. In this paper longitudinal residual strains were compared for autogenous laser welding and laser/ TIG hybrid processes. Joining efficiency which is defined by the penetration depth achieved per unit of energy input was correlated with the residual strain generation. It has been shown that to achieve a specific penetration depth there is an optimum welding condition for each of the welding processes, which will give minimum tensile residual stress generation. The results imply that for the same penetration depth hybrid process resulted in approximately 50% higher tensile longitudinal compared to autogenous laser.

1. Introduction

Control of residual stress and distortion is an important aspect in welding and joining technology. Large longitudinal residual stresses are caused by the compressive plastic flow that occurs in front of the weld pool during the welding thermal cycle. The compressive plastic flow is not balanced by tensile plastic flow on cooling leading to a large tensile residual stresses developing across the weld zone. This tensile zone is balanced by compressive stresses in the surrounding parent material. Distortion is proportional to the area of the tensile peak[1-3]. Distortion is severe in the case of thin components in particular since the compressive stress field can easily exceed the critical buckling load resulting in buckling distortion, the removal of which is expensive and time consuming. There has been done a lot of work on understanding residual stresses and distortions in the past[2, 4, 5]. The most popular methods of minimising welding distortions are post weld rectification, design optimisation and in process manufacturing methods. In addition to these there are some techniques to mitigate distortions during welding, referred to as stress engineering[3, 6-11].

The easiest and the most practical method of reducing residual stress is to use low energy input welding processes such as laser welding. It has been shown that laser welding can produce low distortion joints compared to the traditional arc based welding methods[12]. However, the quality of autogenous laser welds is often insufficient, thus there is a considerable interest in hybrid laser processes. Laser welding can produce efficient welds with a high aspect ratio due to the high energy density of the laser source. However in order to obtain a high quality weld, which is less sensitive to fit-up tolerance the narrow weld produced by laser welding is not always desired, especially in the case of thick sections. On the other hand the hybrid process, where the laser is combined with a conventional arc-based welding, offers better weld quality than autogenous laser welding.

In previous work the synergic effects between laser and arc in hybrid welding were reported[13-17]. However in neither of these

studies laser welding was compared with hybrid welding for the same overall energy input. In this paper the laser welding with 7 kW of power was evaluated against the hybrid welding with the same overall power. Furthermore, the combination of laser and autogenous TIG source enabled a more direct study of heat effects on residual strain magnitude and distribution profile without the influence of filler metal. The use of the fibre laser in this study significantly lowered the susceptibility of the laser beam to be absorbed by the arc plasma.

The aim of this paper was to compare autogenous laser welding with hybrid laser TIG in terms of joining efficiency and magnitude of residual strain for the same applied energy input.

2. Experimental set-up

2.1. Welding

In order to investigate the relationship between weld quality, energy input and residual strain generation a series of laser and hybrid welds were produced. Different sets of welding parameters were used to produce bead-on-plate welds with different aspect ratios and bead characteristics.

The welding conditions can be broadly divided into three groups: laser welding with 4 kW of power, laser welding with 7 kW of power and laser plus TIG hybrid welding with 7 kW of overall power, which included 4 kW from laser and 3 kW from TIG. The latter combination of conditions allows a direct comparison of the laser and the hybrid laser welding at the same energy input. The travel speed was varied between 1-8 m/min for each of the processes. An IPG YLR-8000 CW fibre laser with a maximum power of 8 kW and a fibre diameter of 300 μm was used as the laser source. The laser beam was collimated with a 125 mm focal length lens and focused using a lens with 250 mm focal length. This optical arrangement resulted in a spot size of 630 μm with a top hat energy distribution profile. For all the hybrid welds a Migatronic BDH 550 TIG source was used. The energy input in the TIG process was calculated from the average voltage and current, which were measured by means of Yokogawa DL750 Scope Corder. All tests, including the hybrid trials were carried out without any filler wire. The material used for the investigation was 250x50x12 mm^3 S355 low carbon steel. The specimens were clamped along the whole length and no backing bar was applied. Pure shield argon was used as a shielding medium.

2.2. Residual strain measurement

The objective of this work was to correlate the residual strain generation for different kind of welding processes with a range of energy inputs. Therefore a number of samples were analysed with varying energy input and manufactured using laser and laser plus TIG hybrid process. In welding residual stresses and therefore strains are most significant in the longitudinal direction, which is the same as the welding direction. In the present study longitudinal strain measurement was carried out and compared for different welding processes, as it would give a proportional indication of the longitudinal stress state.

The neutron diffraction experiment was carried out at the ENGIN-X strain scanner at the spallation neutron source at ISIS, RAL, Oxford, UK. The details of ENGIN-X could be found elsewhere[18, 19]. In the present experiment a time of flight range of 20-40 msec was used which resulted into an inter-planar spacing of 1.1 to 2.1 Å. The {110}, {200} and {211} families of crystallographic planes were analysed. An incoming beam dimension of 2 mm × 2 mm was used for the longitudinal strain measurement which allowed

measurement of the strain variation at an appropriate length scale. A 2 mm collimator was used for all the measurements, which resulted in a cuboid gauge volume of 2×2×2 mm^3. The gauge volume was focused 2 mm under the surface of measured specimens. Refinement of the diffraction spectrum was performed using the General Structure Analysis System (GSAS) programme which gave an average lattice parameter (a) of the irradiated volume[20].

3. Joining efficiency

The same penetration depth in laser welding can be obtained with different combinations of parameters, which correspond to different energy input values. Furthermore, for the same energy input different penetration depths can be achieved, particularly in laser welding where different spot sizes can be applied. Gao et al. showed that different welds can be obtained at constant overall energy input if the energy ratio of laser and arc changes[14].

In order to characterise a weld in terms of energy required per millimetre of depth of weld we use the term joining efficiency. Joining efficiency defines how much energy per unit length of a particular process was utilised per unit of penetration depth. Thus the joining efficiency is equal to the ratio of penetration depth and energy input, which in terms of welding parameters corresponds to a ratio of welding speed (**v**) and penetration depth (**D**) to the power (**P**) and is given by equation 1.

$$JE = \frac{v \cdot D}{P} [mm^2 / kJ]$$
(1)

Consequently for a given penetration depth high joining efficiency corresponds to low energy input and in practice should mean low residual stress and distortion. The conditions at which the joining efficiency reaches the maximum ensure welds with the highest aspect ratios of penetration depth to width and with a relatively low energy input. A typical plot of the joining efficiency as a function of travel speed is shown in Fig.1. It can be seen that the joining efficiency initially increases with the travel speed and then after reaching the maximum tends to decrease again. This effect can be explained by the fact that the weld width reduces as the energy input reduces (by increase of the travel speed at constant power). The penetration depth also slightly reduces but the rate of reduction of the weld width is more than the rate of reduction of the penetration depth. Thus as a net result the aspect ratio of weld and the joining efficiency increase in this region. However, at a certain point the weld width reaches a minimum for a given material and any further increase of the travel speed reduces only the penetration depth, without any significant effect on the weld width. After this point the aspect ratio drops and the joining efficiency decreases again with further increase of the travel speed until a point, at which the energy input will be lower than the melting threshold. The maximum joining efficiency is obtained at a point where the heat transfer in to the bulk material (side loses) is minimised, but the process is sufficient to maintain a deep penetration depth.

4. Results

The investigated processes were analysed in terms of the joining efficiency and longitudinal residual strain generation. The results for the joining efficiency are presented in Fig.1. The joining efficiency of the laser welding with 4 kW of power and the hybrid welding with 7 kW of overall power (4 kW laser and 3 kW TIG) reached a maximum at the travel speed of

approximately 4 m/min whereas in the case of the laser welding with 7 kW of power a maximum joining efficiency was obtained at approximately 6 m/min. It can be also seen in Fig.1 that the joining efficiency of the hybrid process was much lower compared with both laser processes.
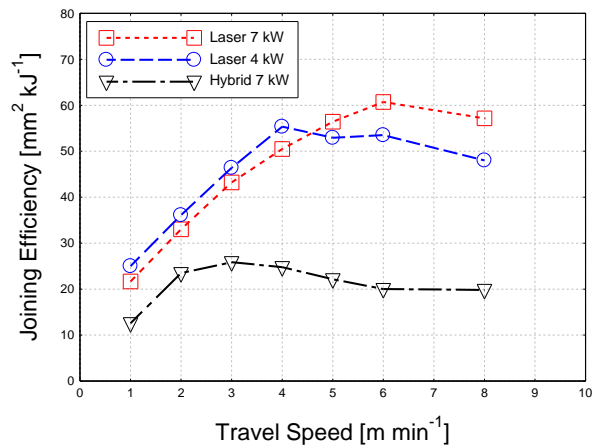

Figure 1: Joining efficiency as a function of travel speed for laser welding with 7 kW of power, laser welding with 4 kW of power and hybrid laser/TIG with 7 kW of overall power (4 kW laser and 3 kW TIG)

On the other hand the best bead quality corresponding to a low sensitivity to fit-up tolerance was obtained in the case of the hybrid process, although no filler wire was used. From the macrographs obtained from the three processes presented in Fig.2, it can be seen that although the hybrid process resulted in a much higher energy input compared to the 4 kW autogenous laser

process the penetration depths obtained for the same travel speed were similar. At all travel speeds the highest penetration depths were obtained in the case of the 7 kW laser process.

The longitudinal strains, measured 2 mm below the top surface of the autogenous laser welds obtained with 7 kW of power as a function of distance from the weld centre line and the travel speeds are plotted in Fig.3. The travel speed seems only to affect the width of the longitudinal tensile strain curve with it reducing as the travel speed increases, whereas the peak magnitude of the tensile strain remains constant. This can be also seen in Fig.4 where the area under the longitudinal tensile strain curve against the travel speed is plotted for all the three processes. There are two important aspects to notice in this figure. Firstly the area of the tensile strain reduces as the travel speed increases. Secondly the tensile strain of the autogenous laser welding with 7 kW of power and the hybrid welding with 7 kW of overall power are similar, whereas in the case of the autogenous laser welding with 4 kW of power the area of the tensile peak is much lower.
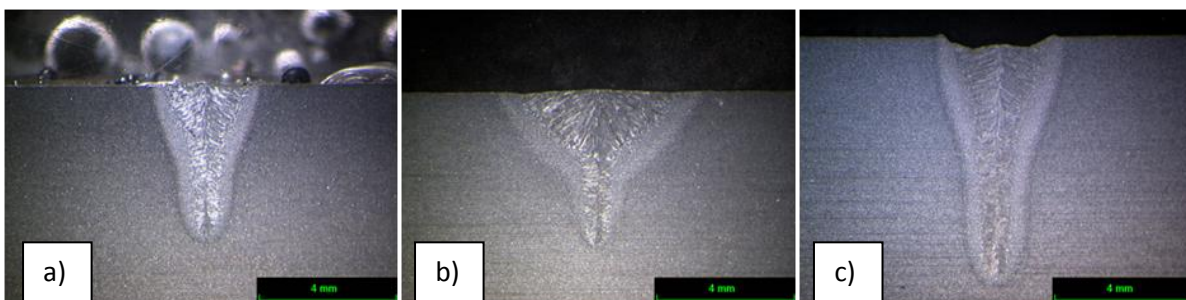

Figure 2: Macrographs of welds obtained at a constant travel speed of 2 m/min; a) laser 4 kW (120 J/mm); b) hybrid 7 kW (210 J/mm); c) laser 7 kW (210 J/mm)
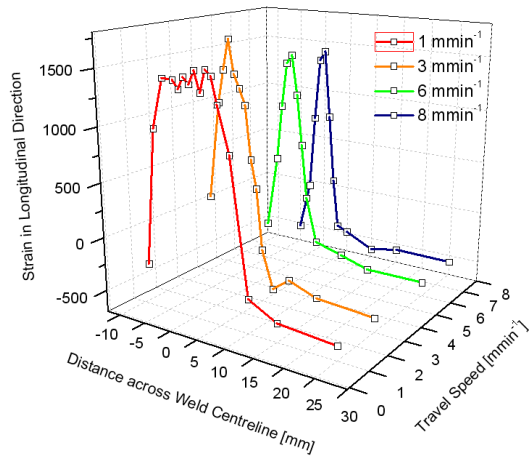
Figure 3: Longitudinal strain profiles measured 2 mm below the top surface as a function of position across the weld centre and travel speed, produced with 7 kW of laser power
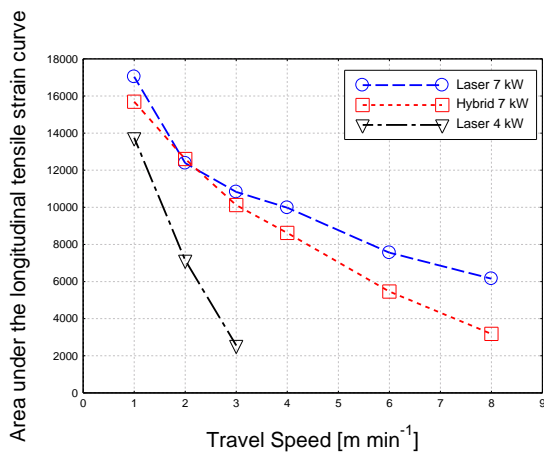

Figure 4: Area under the longitudinal tensile strain curve as a function of travel speed for laser welding with 4 kW of power, laser welding with 7 kW of power and hybrid welding with 7 kW of total power

The reason that there is a difference in the longitudinal tensile strains (Fig.4) between the hybrid and the 7 kW laser process at high welding speeds might result from deterioration of the heat transfer efficiency of the TIG source at high welding speeds. It is worth mentioning that despite the same power (7 kW) being applied in both the autogenous and hybrid processes the penetration depth of the laser welding was almost double that of the hybrid welding.

The reduction of energy input and residual strain with the increase of travel speed occurs irrespectively of the penetration depth. Therefore, the results in the next part are presented in a way to enable a direct comparison of the different welding processes for the same penetration depth. In this test the travel speed was varied for the different processes (laser welding with 4 kW of power, laser welding with 7 kW of power and hybrid welding with 7 kW of overall power) to obtain the same penetration depth. The macrographs presented in Fig.5 show such a comparison for 6 mm of penetration depth. It is worth noticing that the weld obtained at 7 kW (Fig.5c) is narrower that the weld obtained at 4 kW (Fig.5a). The applied energy inputs for 4 kW laser welding, 7 kW hybrid welding and 7 kW laser welding are 240 J/mm, 420 J/mm and 140 J/mm respectively. In Fig.6 the longitudinal strains of the corresponding specimens are plotted. The largest longitudinal tensile strain profile occurs in the case of hybrid weld, whereas the smallest longitudinal strain profile occurs in the laser
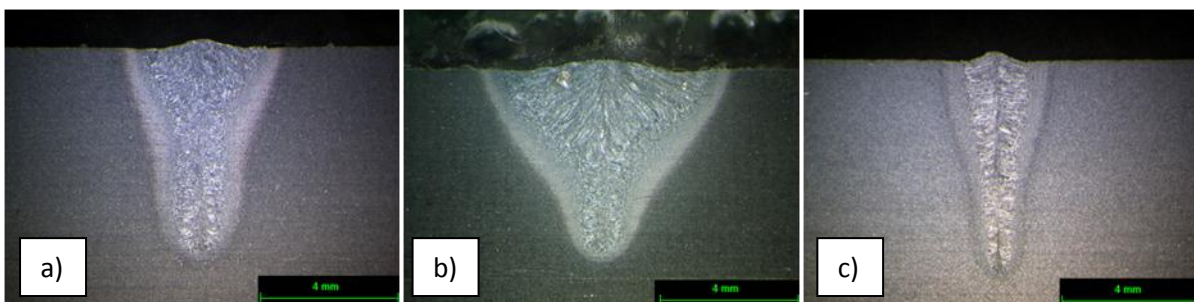

Figure 5: Macrographs of welds of three processes with the combination of parameters required for 6 mm of penetration depth: a) laser welding 4 kW, 1m/min (240 J/mm); b) hybrid welding 7 kW, 1 m/min (420 J/mm); c) laser welding 7 kW, 3 m/min (140 J/mm)
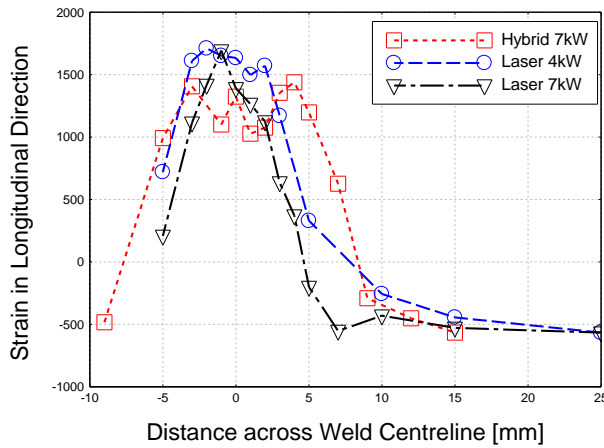
weld obtained at 7 kW of power.

Figure 6: Comparison of the longitudinal strains, measured 2 mm below top surface, between the three processes at constant penetration depth of 6 mm
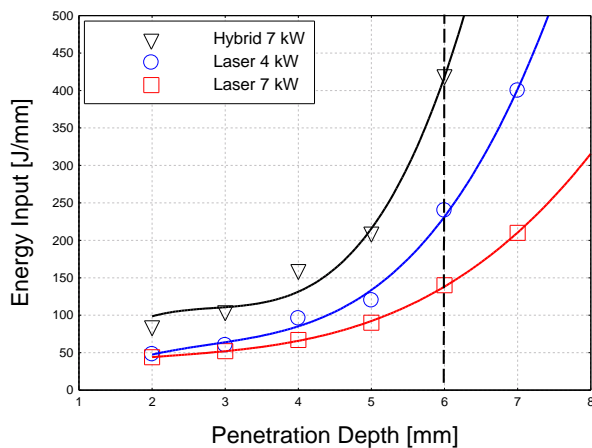

Figure 7: Comparison of joining efficiency as a function of penetration depth between laser welding with 4 kW of power, laser welding with 7 kW of power and hybrid welding with 7 kW of overall power

The applied energy input as a function of penetration depth is shown in Fig.7 (dashed line indicates 6 mm penetration depth). It is clear that the energy input of the hybrid process exceeds that of both autogenous laser processes for the entire range of penetration depths. If both autogenous laser processes are considered (4 kW laser and 7 kW laser) the lower energy input was applied in the case of 7 kW laser process for the analysed 6 mm penetration depth. In general among all tested conditions the 7 kW laser process required the lowest energy for a particular penetration depth with exception for shallow penetration depth where the 4 kW laser process approached the 7 kW process.

5. Discussion

Laser welding is characterised by high energy density with low energy input, which promotes welds with high aspect ratio and joining efficiency. The joining efficiency of the hybrid process is much lower compared to the autogenous laser welding, as shown in Fig.1. This fact can be better understood by analysing the macrographs shown in Fig.2. The penetration depth of the hybrid process with 7 kW of overall power is equal to the penetration depth of laser welding with 4 kW of power. This means that the extra heat from the arc source in the hybrid process did not contribute to the penetration depth, but a large heat source resulting in a large weld width and melting area. The penetration depth of the laser welding with 7 kW of power is almost double than the penetration depth of the hybrid welding using 7 kW of overall power.

The residual strain analysis shows that for a given penetration depth the strain generation is minimised when the joining efficiency is maximised. As the travel speed increases at constant power the amount of heat absorbed in to the workpiece decreases, causing a decrease of the residual tensile strain domain, as shown in Fig4. However, the penetration depth also reduces as travel speed increases.

It is more useful in terms of welding applications to compare different welding processes at the parameters, which are necessary to obtain a particular penetration depth. The macrographs presented in Fig.5 show such an example. The best quality and the lowest sensitivity to fit-up tolerance was

obtained in the hybrid process (Fig.5c). However, the hybrid weld exhibits the highest residual strain from all the three processes (Fig.6). The width of tensile strain domain shown in Fig.6 is the smallest in case of the laser weld with 7 kW. The calculated area under the tensile strain domain shows a 50% reduction in the area in the 7 kW autogenous laser weld compared to the 7 kW hybrid weld. This corresponds to a 50% reduction of the tensile strain in the laser welding compared to the hybrid process for the same penetration depth. A required energy input per unit of penetration depth plotted in Fig.7 clearly shows difference between the processes. Since the arc in the hybrid process did not contribute to the penetration depth this process is less efficient in terms of energy per unit of penetration depth. Comparing both laser processes the 7 kW laser welding was operated in more efficient conditions than the 4 kW laser welding. The high power in this case enabled an increase in welding speed, resulting in a reduction of energy input and residual strain as a result. The laser process with 4 kW of power required a relatively low travel speed in order to achieve the required 6 mm of penetration depth, which resulted in a relatively high energy input and residual strain. Only at shallow penetration depths the joining efficiency of the 4 kW laser process approached the efficiency of 7 kW laser process, because the energy inputs were similar (Fig.7).

It is clear that the choice of welding parameters for a given penetration depth depends on the application requirements. The hybrid process gives a wide weld with a good fit-up tolerance but also results in a larger residual strain field that could lead to issues with distortion. If the residual strain needs to be minimised then a higher laser power should be used.

6. Conclusions:

From the comparison of laser and laser with TIG hybrid welding under the conditions shown in this paper the following can be concluded:

- If you convert a laser process into a hybrid process the extra energy input will result in widening of the weld bead but the penetration depth will not increase.
- This means that, the joining efficiency decreases and the width of the longitudinal strain profile broadens, which could lead to issues with distortion.
- For a particular penetration depth the hybrid process in comparison to the laser process will have a lower joining efficiency and a higher residual strain (equivalent to stress) and broader weld bead profile.
- For large penetration depths higher laser powers and the travel speeds give lower energy input and therefore lower residual strains compared to using lower laser power and travel speed.

References:

1. K. Masubuchi: 'Analysis of welded structures : residual stresses, distortion and their consequences', xi,642p.; 1980, Oxford, Pergamon.
2. D. Radaj: 'Heat effects of welding : temperature field, residual stress, distortion', xxii, 348p.; 1992, Springer.
3. S. W. Williams and A. Steuwer: 'Residual stress in friction stir welding', in 'Friction stir welding. From basics to applications', (eds. D. Lohwasser, et al.), 215-244; 2010, Cambridge UK, Woodhead Publishing Limited.
4. L. E. Lindgren: 'Numerical modelling of welding', *Computer Methods in Applied Mechanics and Engineering*, 2006, **195**(48-49), 6710-6736.
5. L. E. Lindgren: 'Computational welding mechanics : thermomechanical and microstructural simulations '; 2007, Woodhead.
6. J. Altenkirch, A. Steuwer, M. J. Peel, P. J. Withers, S. W. Williams, and M. Poad: 'Mechanical tensioning of high-strength aluminum alloy friction stir welds', *Metallurgical and Materials Transactions A: Physical Metallurgy and Materials Science*, 2008, **39**(13), 3246-3259.
7. J. Altenkirch, A. Steuwer, P. J. Withers, S. W. Williams, M. Poad, and S. W. Wen: 'Residual stress engineering in friction stir welds by roller tensioning', *Science and Technology of Welding and Joining*, 2009, **14**(2), 185-192.
8. F. W. a. K. Brust, D. S.: 'Processes and mechanisms of welding residual stress and distor-

tion, chapter 8: Mitigating welding residual stress and distortion'; 2005, WoodheadPublishing in Materials.

9. D. A. Price, S. W. Williams, A. Wescott, C. J. C. Harrison, A. Rezai, A. Steuwer, M. Peel, P. Staron, and M. Koçak: 'Distortion control in welding by mechanical tensioning', *Science and Technology of Welding and Joining*, 2007, **12**(7), 620-633.
10. V. A. Vinokurov: 'Mechanical aspect of stress relieving by heat and non-heat treatment. In Stress Relieving Heat Treatments of Welded Steel Constructions.'; 1987, Sofia, Bulgaria,
11. W. Soete: 'Measurement and relaxation of residual stresses', *Welding Journal*, 1949, **28**(8), 354s-364s.
12. P. Colegrove, C. Ikeagu, A. Thistlethwaite, S. Williams, T. Nagy, W. Suder, A. Steuwer, and T. Pirling: 'Welding process impact on residual stress and distortion', *Science and Technology of Welding and Joining*, 2009, **14**(8), 717-725.
13. Y. B. Chen, Z. L. Lei, L. Q. Li, and L. Wu: 'Experimental study on welding characteristics of CO_2 laser TIG hybrid welding process', *Science and Technology of Welding and Joining*, 2006, **11**(4), 403-411.
14. M. Gao, X. Y. Zeng, Q. W. Hu, and J. Yan: 'Weld microstructure and shape of laser-arc hybrid welding', *Science and Technology of Welding and Joining*, 2008, **13**(2), 106-113.
15. B. Hu and G. Den Ouden: 'Synergetic effects of hybrid laser/arc welding', *Science and Technology of Welding and Joining*, 2005, **10**(4), 427-431.
16. Y. P. Kim, N. Alam, and H. S. Bang: 'Observation of hybrid (cw Nd:YAG laser+MIG) welding phenomenon in AA 5083 butt joints with different gap condition', *Science and Technology of Welding and Joining*, 2006, **11**(3), 295-307.
17. B. Ribic, R. Rai, and T. DebRoy: 'Numerical simulation of heat transfer and fluid flow in GTA/Laser hybrid welding', *Science and Technology of Welding and Joining*, 2008, **13**(8), 683-693.
18. M. W. Johnson, L. Edwards, and P. J. Withers: 'Engin - A new instrument for engineers', *Physica B: Condensed Matter*, 1997, **234-236**, 1141-1143.

19. J. R. Santisteban, M. R. Daymond, J. A. James, and L. Edwards: 'ENGIN-X: A third-generation neutron strain scanner', *Journal of Applied Crystallography*, 2006, **39**(6), 812-825.

20. A. C. Larson and R. B. von Dreele: 'General Structure Analysis System (GSAS), LAUR 86-748', Los Alamos National Laboratory, Los Alamos, NM, USA, 1994.